A Study of the Relative Barrel and Endcap Alignment of the CMS Muon System

Siddharth Mishra Sharma

University of Cambridge
E-mail: sm806@cam.ac.uk

Supervisors: Luca Scodellaro and Teresa Rodrigo

Instituto de Física de Cantabria
CERN

Abstract: A study of the relative alignment between the barrel and endcap components of the muon system at the Compact Muon Solenoid (CMS) is presented. By extending a technique previously used to validate internal barrel alignment, a method involving segment extrapolation is developed such that segments reconstructed in the DT (Drift Tube) chambers on the outer wheels of the barrel are extrapolated to the CSCs (Cathode Strip Chambers) in the inner endcap stations to test alignment. The accuracy of extrapolation is ascertained by applying the method to a Monte Carlo simulation with ideal geometry. The method applied to current (as of August 2011) and proposed detector geometry reveals possible residual misalignments. Corrections subsequently applied to the current geometry produce a significantly better alignment scenario. This report summarizes work done at CERN as part of the Summer Student 2011 program.

Contents

1. Introduction

The unprecedented complexity of the tracking components in the Compact Muon Solenoid (CMS), a multi-purpose particle detector located at CERN, requires that they must be aligned to a high precision to ensure optimum performance. Deviations from ideal geometry (misalignments) may arise due to several factors including limited mounting precision of the sensor modules, magnetic/thermal stresses and changes in environment, which may be time dependent. These degrade the quality of muon identification and track reconstruction, and further necessitate the design and implementation of precise alignment techniques.

A detailed description of the detector and it's physics goals, which include discovering the Higgs boson and finding evidence of physics beyond the standard model, can be found in [1, 2]. In order to successfully meet these goals, it is necessary that the detector have the ability to identify and resolve muons over a wide range of momenta and angles. Good muon identification resolution is of central importance in the analysis of CMS data because it enables the recognition of several interesting processes. A typical example is the predicted decay of the Higgs boson into ZZ or ZZ^*, which in turn decay into 4 leptons. For the case in which all leptons are muons, the decay has been called "gold plated".

The aim of this project is to study the relative alignment between the major components of the muon system, the barrel and the two endcaps. In doing so it will be possible, after developing the necessary tools, to observe any possible biases between the components.

2. Geometry of the Muon System

A transverse slice through CMS is shown in Figure 1, in which the major layers can be discerned. Central to this project is the outermost layer – the muon system. A longitudinal section through one quarter of the muon system is shown in Figure 3. The barrel is subdivided into 5 wheels (0, $\pm$1 and $\pm$2) with 4 concentric stations (MB1, MB2, MB3 and MB4), while the endcaps each contain 4 stations (ME$\pm$1, ME$\pm$2, ME$\pm$3 and ME$\pm$4) with 1 to 3 rings in each station.

The system uses three types of gaseous chambers for muon detection. The Drift Tube (DT) chambers are located in the barrel and positioned parallel to the beamline. Distinct wire layers in the chambers measure the muon position in the $r\phi$ bending plane and in the z direction along the beamline. Similarly, Cathode Strip Chambers (CSCs) are located in the two endcap regions of the detector. These are located in 4 stations in each endcap and positioned perpendicular to the beam line. Resistive Plate Chambers (RPCs) located in the barrel and endcaps provide a fast and independent triggering system which complements the CSCs and DTs in efficient background rejection, track selection and identification over the entire p_T range.

The global coordinate system (Figure 1) is common to all the components. The Z axis is along the clockwise beam line, the X axis points to the center of the LHC ring and the Y axis is directed in accordance with the right hand rule. Local coordinate systems (x, y, z) are also defined for the individual muon chambers (Figure 2).

Several techniques are used to align the CMS muon system. For the bulk of this study hardware-aligned geometry is used for the barrel and geometry using track-based alignment for the endcap. Hardware alignment uses an optical system to align the chambers, while track-based alignment uses tracks extrapolated from the central silicon tracker. A description of alignment systems can be found in [4] for hardware alignment and [3] for track-based alignment.

3. Method: Segment Extrapolation

For a given track, compatible segments are matched to it by requiring that the track hit belong to the chamber of the segment. CSC and DT chambers from the track are then associated with each other to form a barrel and endcap segment pair.

Segments reconstructed in the DT chambers of the barrel are then extrapolated to the the CSCs in the endcap. Details of the extrapolation process can be found in [3]. A minimum number of 3 chamber hits and a p_T cut of 20 GeV are imposed as selection criteria to reduce the effects of multiple scattering and relatively poorly described magnetic field in the barrel-endcap overlap region and ensure good tracks. To ensure minimum error

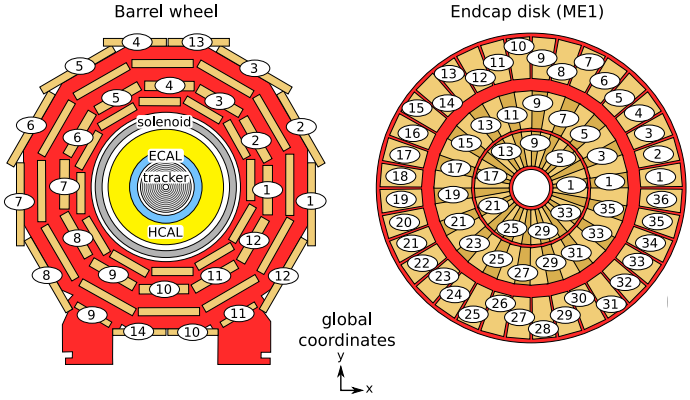

Figure 1: Transverse slice through the central barrel wheel and inner endcaps showing chamber positions and global coordinates.

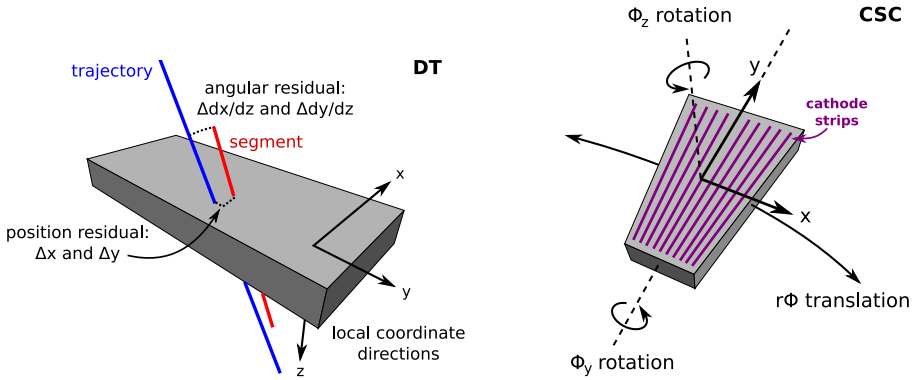

(a) Residuals and local coordinates of a drift tube chamber.

(b) Geometry and local coordinates of a cathode strip chamber.

Figure 2: Chamber geometry

propagation in extrapolation across larger distances, segments in the ± 2 wheels of the barrel and the corresponding ± 1 stations of the endcap are used. The DT segments extrapolated to the endcap can be compared to the segments reconstructed in the CSC chambers by plotting the distribution of residuals. Residuals are plotted for x, y, $\frac{\mathrm{d}x}{\mathrm{d}z}$ and $\frac{\mathrm{d}y}{\mathrm{d}z}$ for local coordinates and a similar set of variables for global coordinates.

Several propagation effects contribute to the expected shape of the residual distribution; these are discussed in detail in [3]. In summary, we expect the statistical errors in extrapolation to produce a Gaussian distribution in the limit of the central limit theorem, with other effects contributing to a non-Gaussian tail. The standard deviation of the distribution is indicative of the resolution of detection of the respective coordinate. Any systematic misalignments can be seen as a deviation of the mean from zero (within the limits of sensitivity of extrapolation).

From the description of coordinate systems (Figures 1 and 2) we see that biases in global X and Y point to global shifts, in local x to relative rotation around global Z and

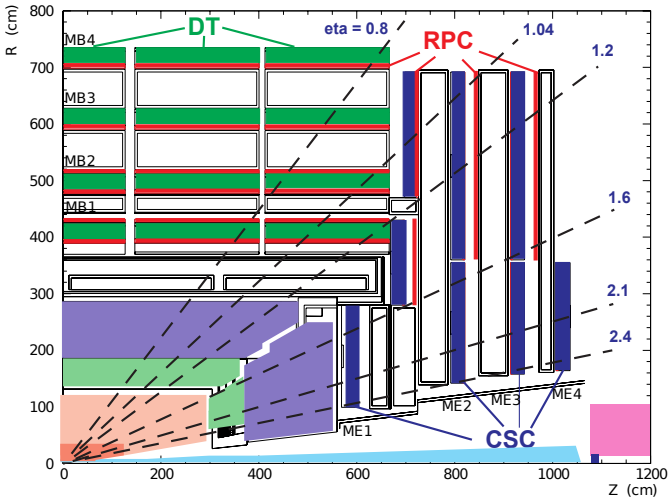

Figure 3: Longitudinal slice through a quarter of the muon system.

in local y to radial misalignment (e.g. relative expansion) or shift in global Z.

4. Monte Carlo Study

In order to test the extrapolation algorithm and characterize the extrapolation sensitivity, a Monte Carlo collision simulation (QCD MuEnriched) was used and segments were reconstructed using ideal detector geometry.

4.1 Residual Distributions

The resulting residual means are summarized in Table 2 and residual distributions shown in Figure 9. Complete residual distribution plots are placed in Appendix A.

The magnitude of deviation from zero of the mean of the distribution can be taken as the accuracy of our technique for the respective variables for the purpose of this study. Values within the required resolution for the x coordinates and global Y coordinate confirm that the extrapolation is working as expected. Large values for local y are observed, possibly due to the inclination of tracks, and motivate a study of residuals as a function of pseudorapidity.

4.2 Pseudorapidity Dependence

The pseudorapidity (η) was computed from the inclination of the DT segments. We can expect it to be a good approximation to the initial η however because ideally the magnetic field acts to change the momentum of the muon in the tranverse directions. For the same reason we expect the η values to be similar for a given DT/CSC segment pair. From Figure 3 we expect tracks passing through both the barrel and endcap chambers to have a pseudorapidity range of approximately $0.9 < |\eta| < 1.2$. The actual distribution obtained from MC is shown in Figure 4. We observe a small number of tracks outside the expected range, perhaps because η was calculated from the DT segment.

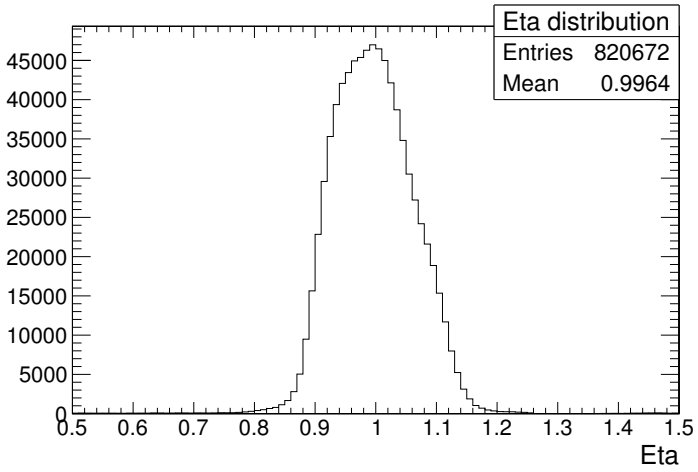

Figure 4: Distribution of η in MC.

To quantify the extrapolation as a function of η we plot the residual distribution for four different eta ranges in Figure 5. It can be seen that the distribution of y residuals is a very strong function of η. This maybe due to imperfect segment reconstruction or extrapolation. No cuts on η are imposed on the studies that follow because the small number of events outside the expected range do not significantly alter the mean in local x and global X and Y, which are the coordinates we shall concentrate on.

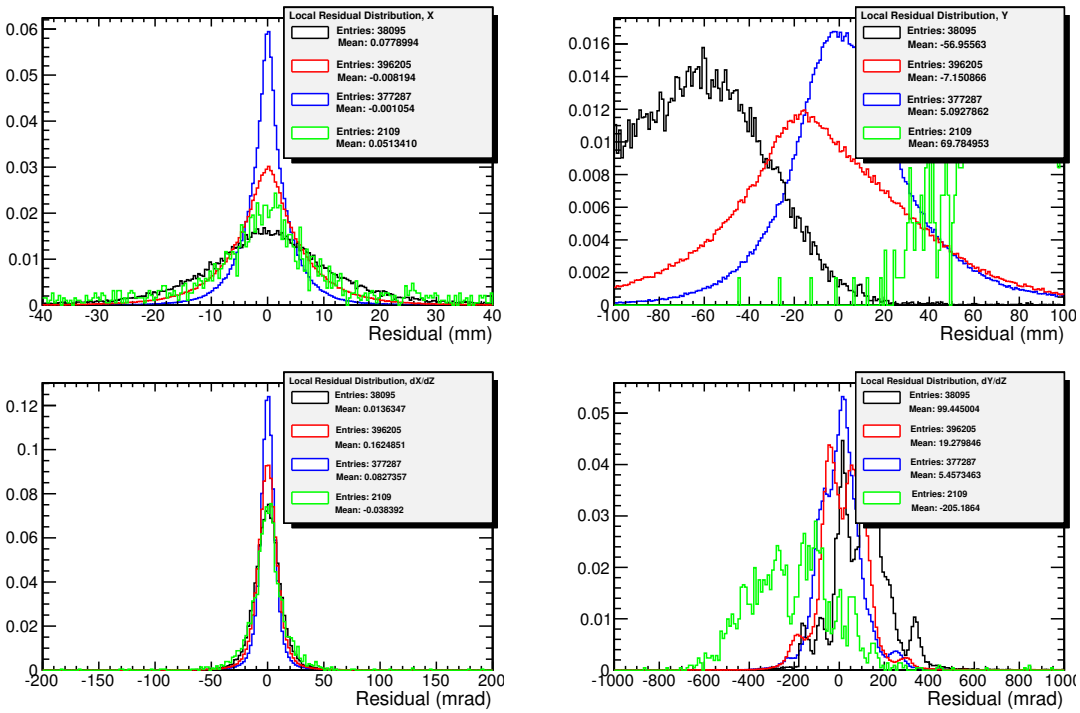

Figure 5: Residual distributions for η ranges (top to bottom on legend): $0.8 < |\eta| < 0.9$, $0.9 < |\eta| < 1.0$, $1.0 < |\eta| < 1.2$, $1.2 < |\eta| < 1.4$.

5. Studies on Data

5.1 A Preliminary Test on Previous Geometries

A preliminary study was performed comparing two different geometries – PromptReco-v1 geometry from November 2010 with twisted tracker geometry and PromptReco-v4 twist-free geometry from March 2011. The data used was SingleMu/Run2011A-PromptReco-v*.

In the November 2010 geometry, a weak mode in tracker track-based alignment caused a ϕ misalignment linearly growing with Z. This causes the endcap chambers, which are aligned by extrapolating tracks from the tracker, to be "twisted" in opposite ϕ directions with respect to the barrel. The barrel itself was not affected by the tracker twist because it was aligned using the optical system rather than extrapolated tracks.

Hence, we expect a twist in the tracker for v1 geometry to appear as a bias in local x, as seen in Figure 6. The above analysis further validates our extrapolation technique, allowing us to look at residuals from recent geometry in greater detail.

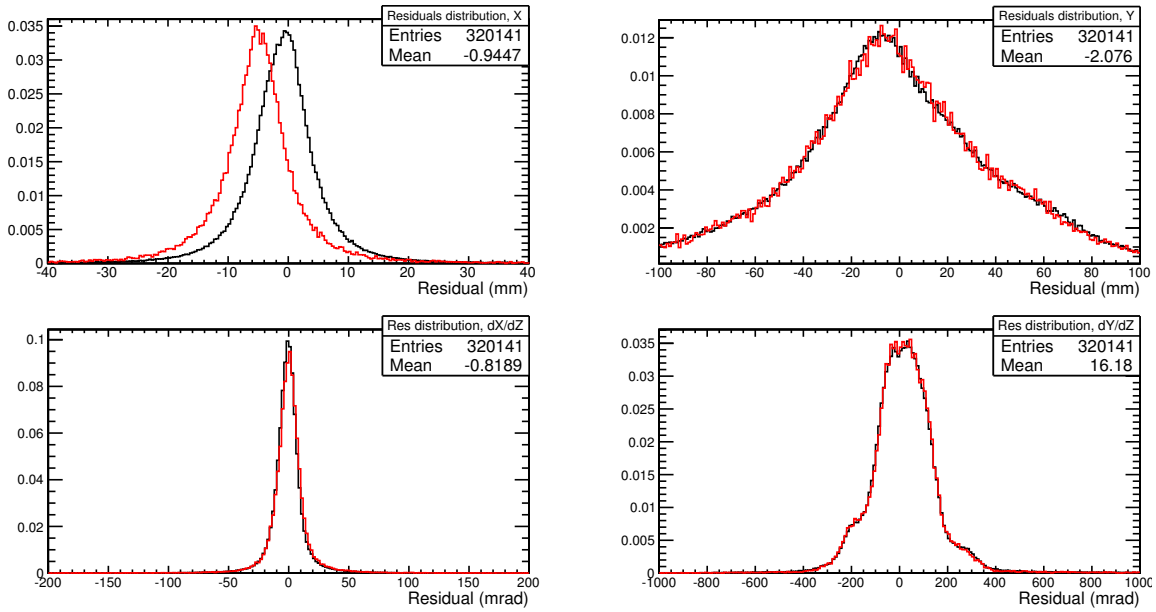

Figure 6: Comparison of residual distributions for twisted (red) and twist-free (black) geometry. All plots normalized.

5.2 Geometry With Hardware Barrel Alignment

The extrapolation was applied to data with PromptReco-v4 (current as of August 2011) geometry. A summary comparison between MC and data residuals for the x coordinate is given in Figure 7 and the full residual plots are in Figure 10.

In general the results reproduce trends shown by the Monte Carlo simulation, with several differences. The residual means for x in local coordinates and X and Y in global coordinates are $\mathcal{O}(100\ \mu\text{m})$ for endcap -1, indicating a possible small relative misalignment. A bias is especially seen for endcap $+1$, with means of over 1 mm in all relevant coordinates. For local x, deviations from the expected shape of the distribution are also observed.

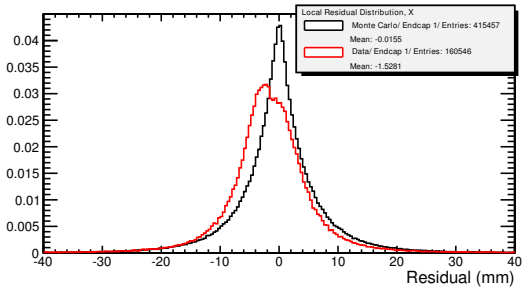

(a) Endcap +1, Local

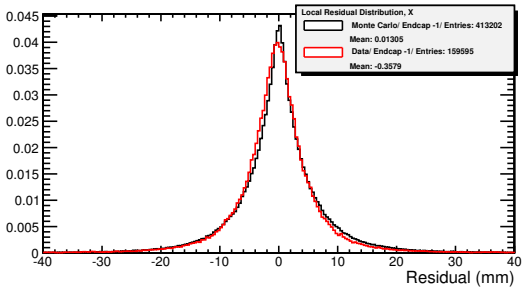

(b) Endcap −1, Local

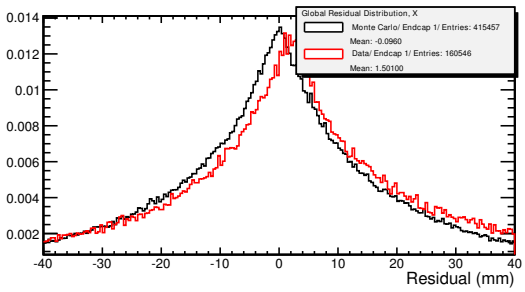

(c) Endcap +1, Global

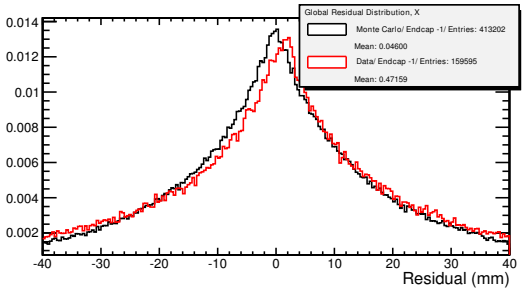

(d) Endcap −1, Global

Figure 7: Ideal Monte Carlo vs. data residual comparison by endcap.

5.3 Geometry with Track-Based Barrel Alignment

By using barrel geometry with track-based alignment, it is possible to further elucidate the bias in local x mentioned in the previous section. Track-based alignment relies on determining the chamber position which minimizes the residuals between locally reconstructed segments and the extrapolated trajectory of candidate muons reconstructed in the tracker. Since in this case both the barrel and endcap chambers are aligned using the same method, any relative bias is expected to be correlated between them and the residual mean is expected to reduce.

The results are summarized in Table 2. The local x residual distribution shows significantly reduced means compared to those shown by hardware-aligned barrel geometry of the previous section for both endcaps and is presented in Figure 8. Complete residual plots are in Figure 12.

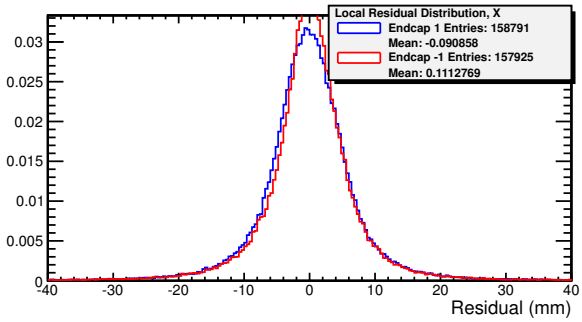

Figure 8: Local x residual distribution for geometry with track-based barrel alignment.

5.4 Corrected Geometry

In order to test the misalignments measured above, we apply corrections consisting of shifts in global X and Y and rotations about global Z (equivalently, shifts in local x) inferred from the local/global residual means for the current geometry to ring 3 of the endcap geometry. We expect a reduction in residual means. The corrections are summarized in Table 1.

	Endcap +1	Endcap −1
Global shift in X	-1.5 mm	-0.5 mm
Global shift in Y	-2.2 mm	-0.9 mm
Global rotation about Z	250 μrad	67 μrad

Table 1: Corrections applied to current geometry.

The obtained residual distributions for the corrected geometry are shown in Figure 11 and the residual means in Table 2. The results are to be compared with those obtained in Section 5.2 for uncorrected geometry. We see significantly smaller means for local x, global X and global Y as well as a healthier overall shape of the distribution for local x in +1.

		Local		Global	
Sample	Endcap	$\overline{\Delta x}$ (mm)	$\overline{\Delta y}$ (mm)	$\overline{\Delta \mathrm{X}}$ (mm)	$\overline{\Delta \mathrm{Y}}$ (mm)
Monte Carlo	+1	−0.015	−2.530	−0.104	−0.151
	−1	0.014	−2.700	0.041	−0.151
Data (uncorrected)	+1	−1.525	−2.117	1.498	2.072
	−1	−0.373	−1.937	0.469	0.860
Data (TB barrel)	+1	−0.091	−1.431	1.087	1.180
	−1	0.111	−1.185	0.236	0.969
Data (corrected)	+1	−0.198	2.169	0.529	0.178
	−1	0.041	−1.838	0.143	0.083

Table 2: Summary of residual means.

5.5 New Geometry

A new set of alignment conditions are due to be implemented to reprocess data collected by CMS in 2011. As an example of the applications of this project, we use segment extrapolation to study the new geometry and compare it to the current (as of August 2011) geometry.

To compare the new muon geometry to the current one, we plot residuals for the updated and current barrel geometry, using the current tracker geometry for endcap alignment. From the results, summarized in Table 3 and Figure 13, we see that the new geometry, benefitting from the larger statistics used to align the chambers, shows an improved global alignment, especially in global X.

We also plot residuals for the updated barrel geometry, seperately using current and new tracker geometries for endcap alignment. In doing so we are indirectly comparing the two tracker geometries, since they dictate global positioning and endcap alignment. Residual means are summarized in Table 3 for endcap +1 and distributions shown in Figure 14. We see a larger residual mean in local x when using the new tracker geometry to align the endcaps, which is indicative of a more pronounced twist in the new tracker geometry.

		Local	Global	
Geometry	Endcap	$\overline{\Delta x}$ (mm)	$\overline{\Delta \mathrm{X}}$ (mm)	$\overline{\Delta \mathrm{Y}}$ (mm)
New muon, current tracker	+1	−1.234	−0.046	2.176
New muon, new tracker	+1	−1.713	−0.076	1.975
Current muon, current tracker	+1	−1.696	1.803	2.170

Table 3: Residual means for the new muon geometry, comparing current and new tracker geometries.

6. Summary and Conclusions

A technique based on segment extrapolation was designed and implemented to test the relative alignment between the barrel and endcaps of the CMS muon system. The sensitivity of extrapolation was ascertained by applying the method to a Monte Carlo simulation with ideal geometry, and is presented in terms of residual means in Table 2.

The method applied to current detector geometry reveals possible residual misalignments between the barrel and endcaps, being especially evident for endcap +1. Corrections subsequently applied produce parameters more consistent with an aligned geometry. Application of the method to compare the proposed and current geometries reveals an improved global position and a slightly more twisted tracker in the proposed geometry.

References

[1] CMS collaboration, *The CMS experiment at the CERN LHC*, 2008 JINST **3** S08004.

[2] CMS collaboration, *CMS Physics Technical Design Report Volume I: Detector Performance and Software*, CERN Report CERN/LHCC 2006-001 (2006).

[3] CMS collaboration, *Alignment of the CMS muon system with cosmic-ray and beam-halo muons*, 2010 JINST **5** T03020.

[4] CMS Collaboration, *Aligning the CMS Muon Chambers with the Muon Alignment System during an Extended Cosmic Ray Run*, 2010 JINST **5** T03019.

A. Appendix: Residual Distributions

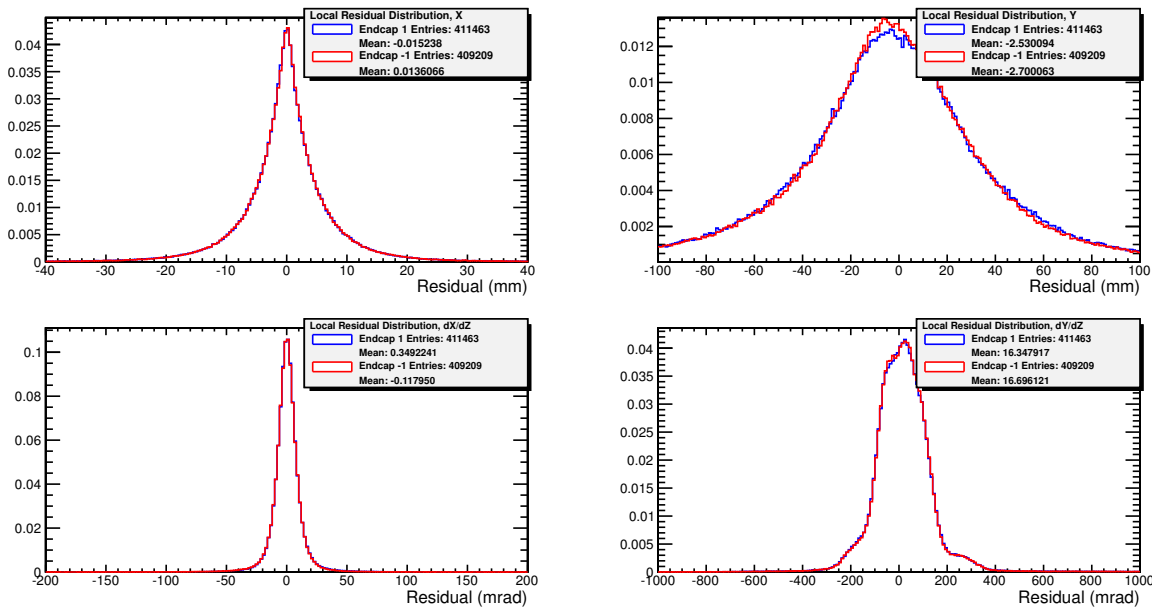

(a) Local Coordinates

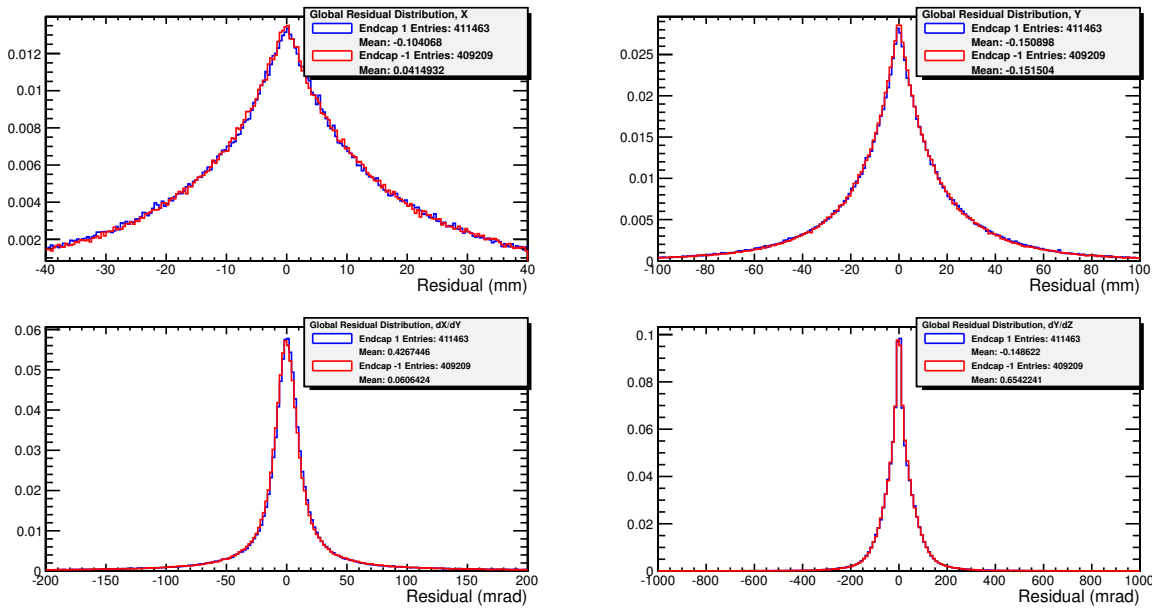

(b) Global Coordinates

Figure 9: Residuals for Monte Carlo simulation with ideal geometry.

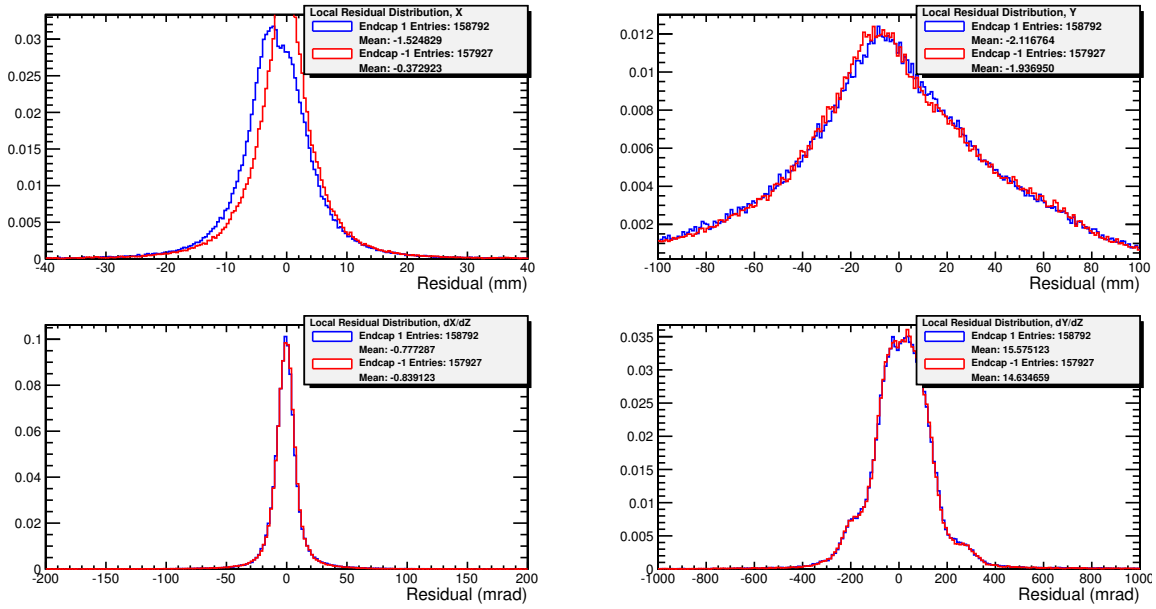

(a) Local Coordinates

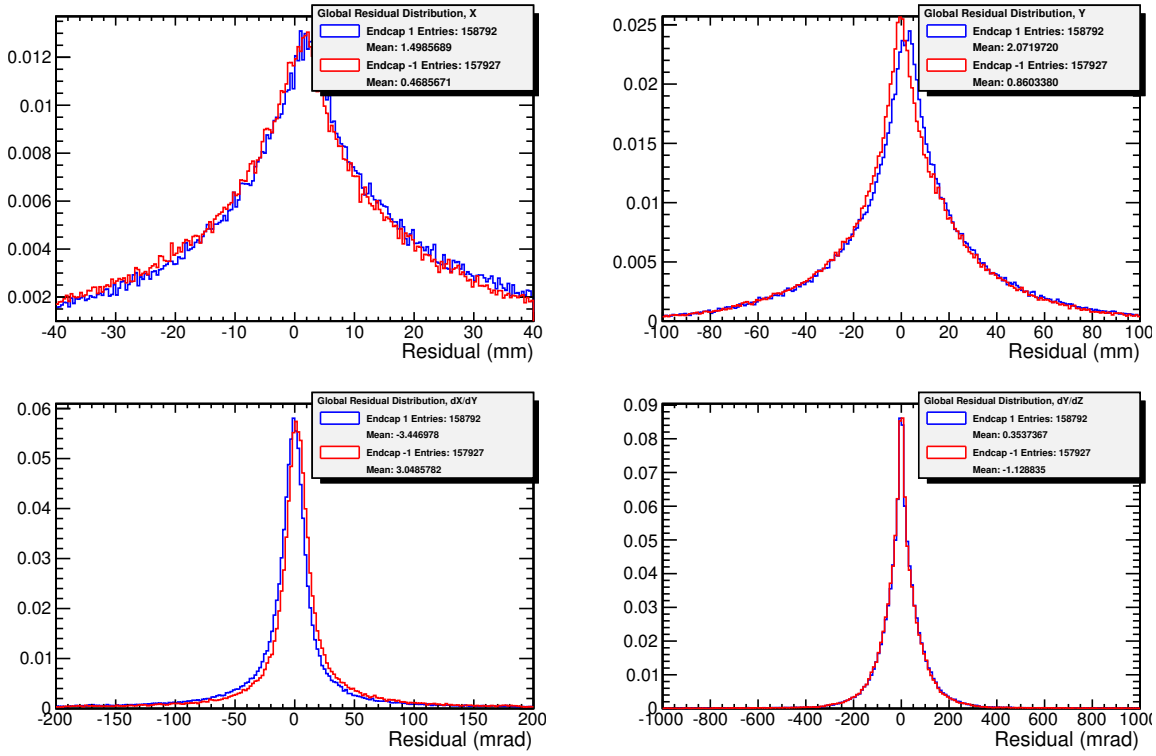

(b) Global Coordinates

Figure 10: Residuals for data with current geometry.

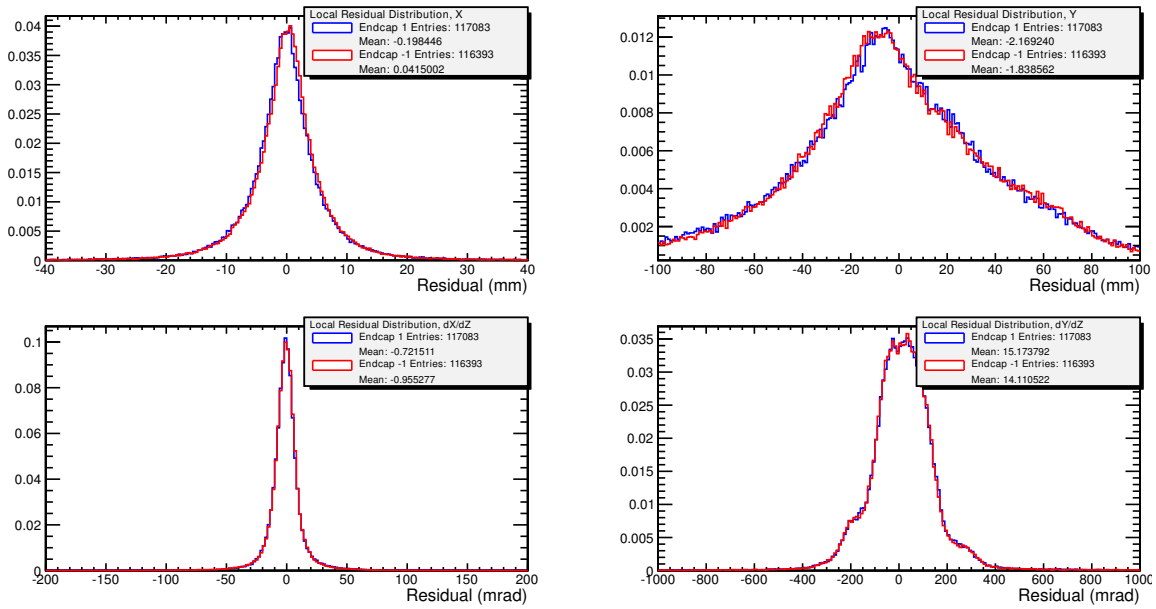

(a) Local Coordinates

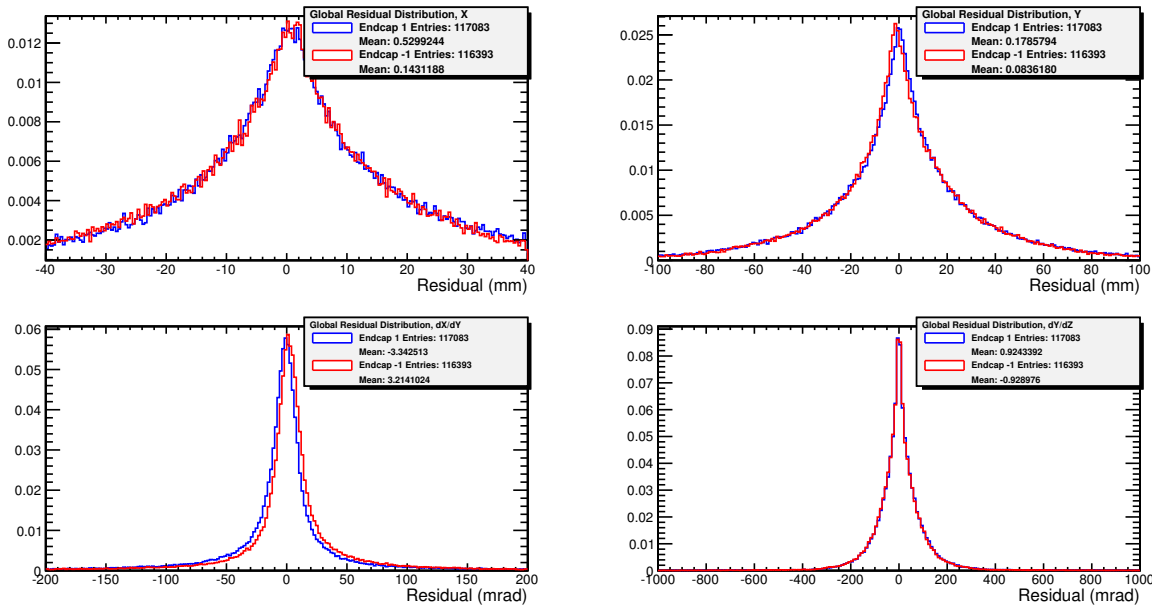

(b) Global Coordinates

Figure 11: Residuals for data with the corrected geometry.

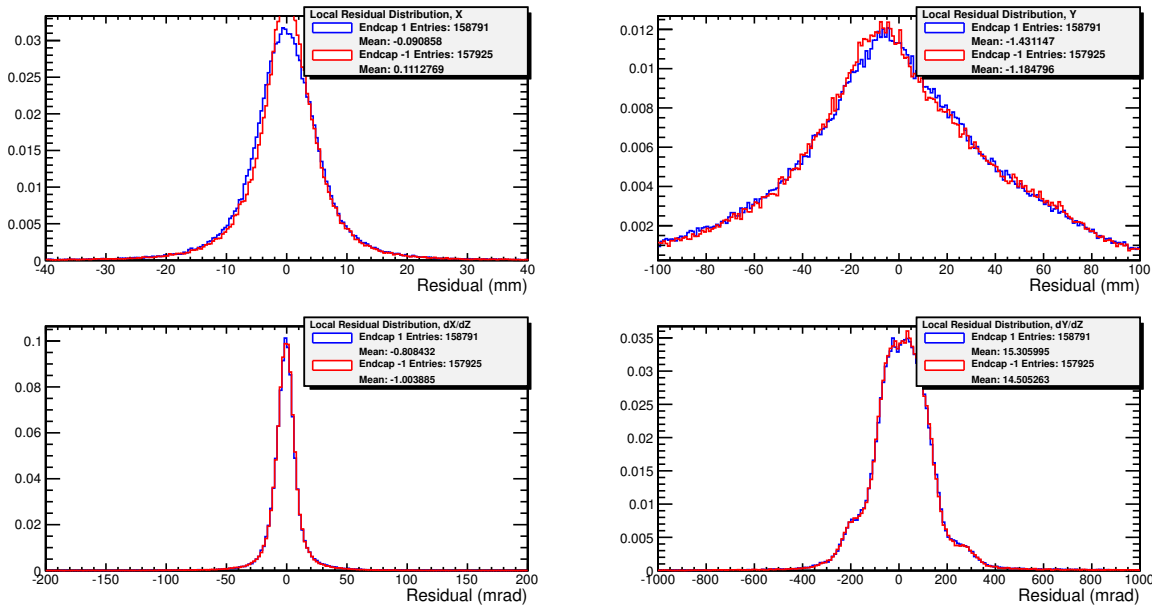

(a) Local Coordinates

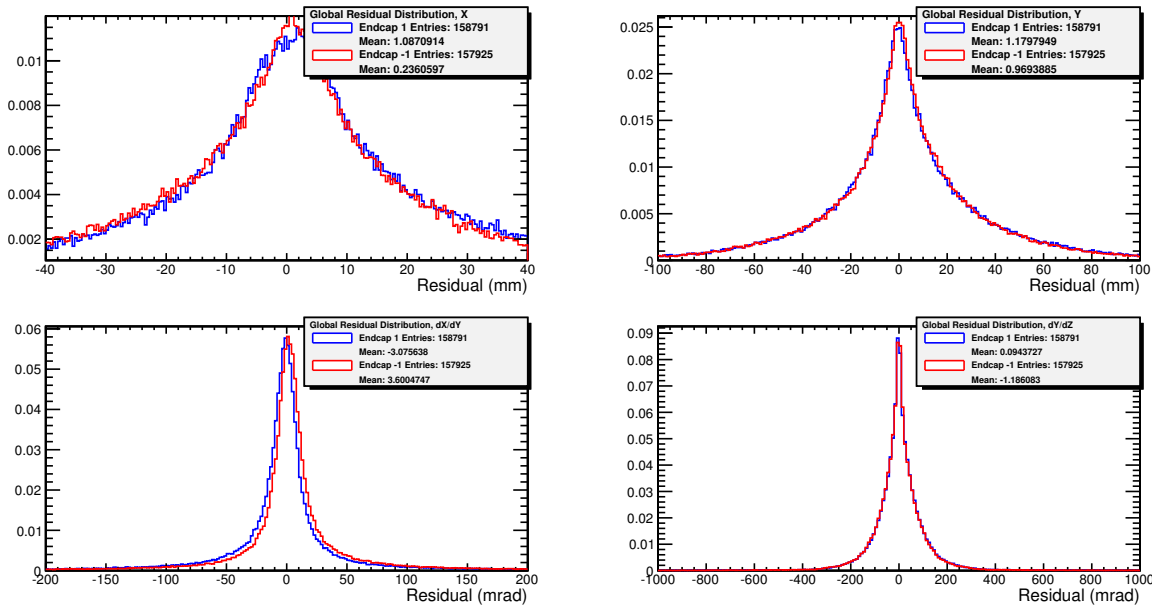

(b) Global Coordinates

Figure 12: Residuals for data with the track-based barrel geometry.

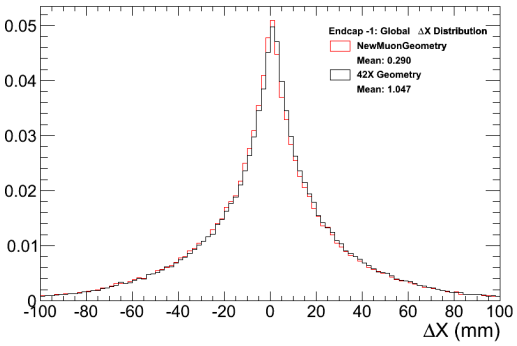

(a) Global X, Endcap -1

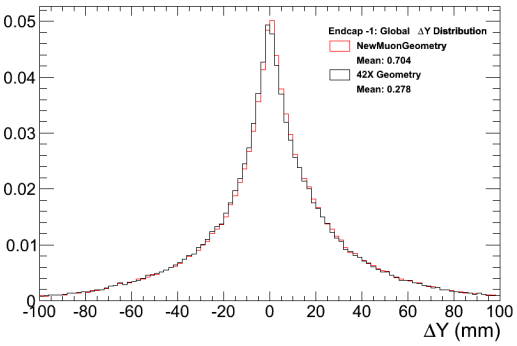

(b) Global Y, Endcap -1

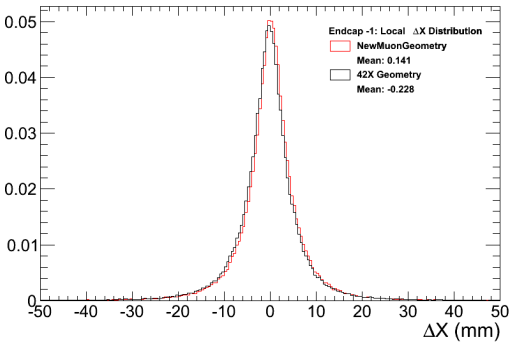

(c) Local x, Endcap -1

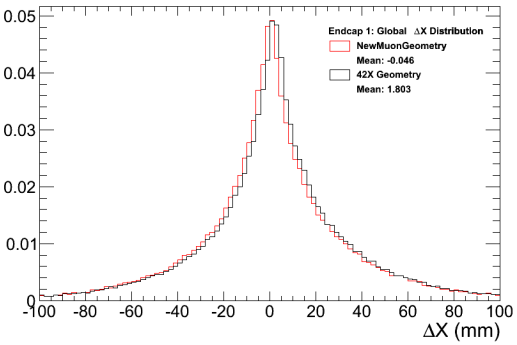

(d) Global X, Endcap +1

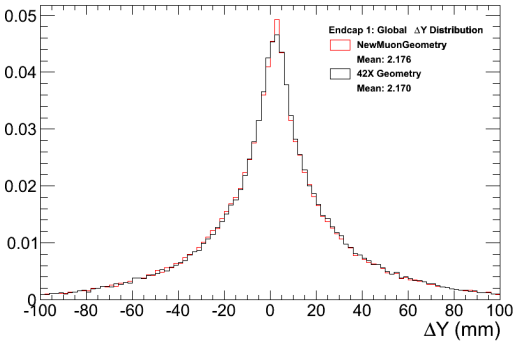

(e) Global Y, Endcap +1

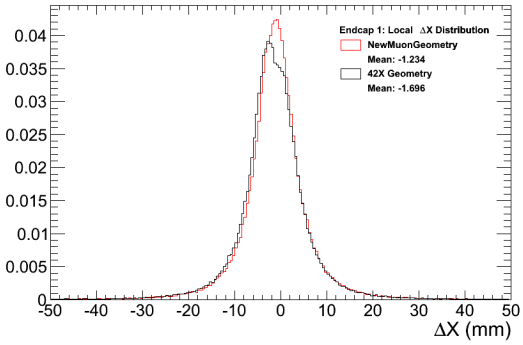

(f) Local x, Endcap +1

Figure 13: Residuals comparing updated and current barrel geometry (using current tracker geometry for endcap alignment). 42X represents the current geometry.

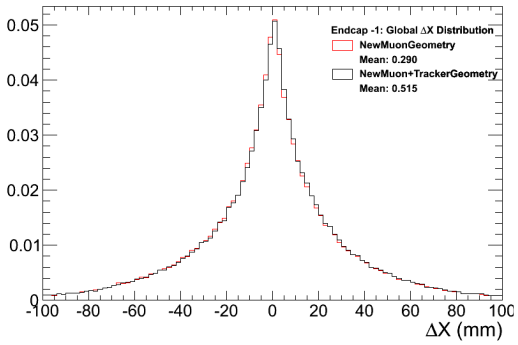

(a) Global X, Endcap -1

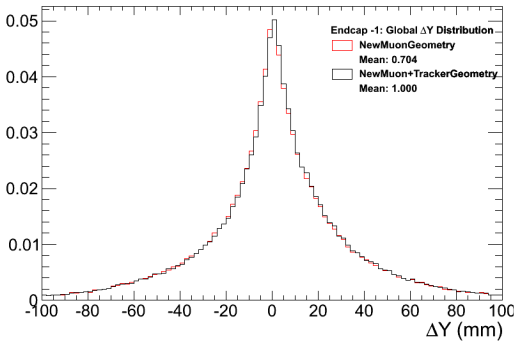

(b) Global Y, Endcap -1

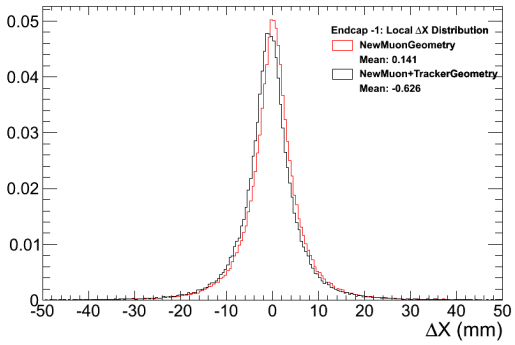

(c) Local x, Endcap -1

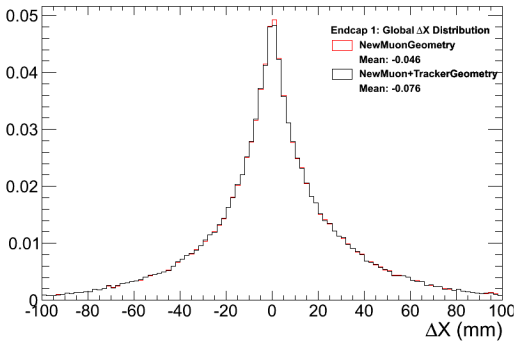

(d) Global X, Endcap +1

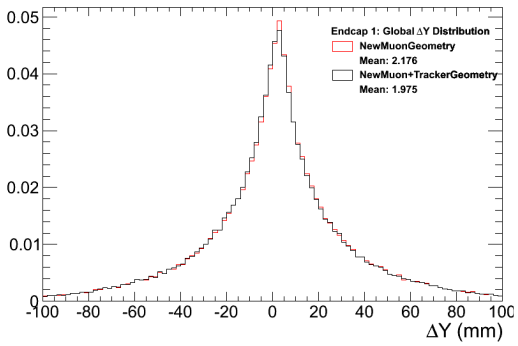

(e) Global Y, Endcap +1

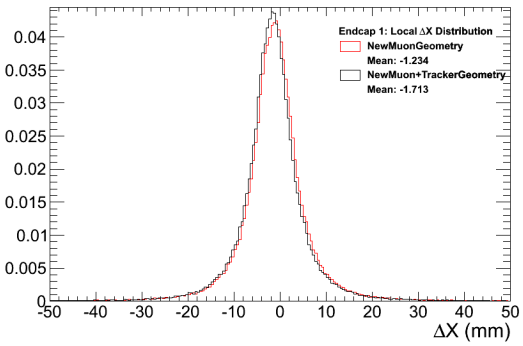

(f) Local x, Endcap +1

Figure 14: Residuals using new and current tracker geometry for endcap alignment, with updated barrel geometry.